

# Instabilities of off-centered vortices in a Bose-Einstein condensate

Tomoya Isoshima,\* Jukka Huhtamäki, and Martti M. Salomaa  
*Materials Physics Laboratory, Helsinki University of Technology,  
P. O. Box 2200 (Technical Physics), FIN-02015 HUT, Finland*  
(Dated: October 31, 2018)

We study numerically the excitations of off-centered vortices in a Bose-Einstein condensate. The displacement of a single vortex and the separation of a doubly quantized vortex are considered. We find that the core-localized excitations of the precessing vortices continue to feature the property which implies that the vortices are unstable. The core-localized, dipolar, and quadrupolar excitations are found to deform continuously as functions of vortex displacements and intervortex separation.

PACS numbers: 03.75.Lm, 03.75.Kk, 67.40.Vs

## I. INTRODUCTION

Quantized vorticity which accompanies rotational motion is a characteristic feature of superfluids. Vorticity involves singular lines, vortex lines which exist inside any closed path enclosing finite circulation. The change in the phase of the order-parameter field around the vortex line is quantized in integer units of  $2\pi$ .

In a Bose-Einstein condensate (BEC) of an atomic gas [1], the first vortex was created by the JILA group [2]. They used a two-component condensate of  $^{87}\text{Rb}$  atoms and imprinted a phase winding of  $2\pi$  onto one component. The position of the vortex core was clearly seen and also the precessional motion of the core was observed [2, 3]. In a one-component condensate, the ENS group [4] created a vortex state using a rotating trap which consists of an optical spoon and a magnetic trap. Condensates containing up to 4 vortices were observed. Their method can be understood in analogy with fluid motion in a rotating vessel. The idea of a rotating trap has been employed by many groups thereafter.

In addition to these singly quantized vortices, multiply quantized vortices with phase windings  $4\pi$  and  $8\pi$  can also be formed [5], using a topological method introduced by Nakahara *et al.* [6]. However, the experimentally recorded image of the cloud of atoms does not show any indications for the splitting of multiply quantized vortices. This surprising apparent stability contradicts with what has been widely expected [1, 7]. Therefore, it is urgent to understand the stability of these off-centered vortices and the multiply quantized vortices.

The axisymmetric and rotationally symmetric (singly quantized) vortex states have been studied and a core-localized excitation with negative excitation energy is found [8, 9, 10, 11, 12, 13]. Concerning this excitation, a relation to the instability of a vortex state [10, 13] (through the transfer of the population from the condensate mode to the core-localized excitation) and also to the precession motion [14, 15] of the vortex core have been pointed out. Nevertheless, the axisymmetric and

rotationally symmetric systems only mimic the experimental situations because (a) the axisymmetric vortex state can become a vortexfree state only through the off-centered vortex states. (b) a system with a vortex under precessional motion is no longer axisymmetric.

The understanding of the excitation level with negative energy involves a puzzling feature [16] because the value is connected to both the direction and frequency of the precession motion and the instability of the vortex state. These two cannot be divided as long as we study the axisymmetric state. Therefore, investigations of the off-centered vortex state are necessary in order to understand both the instability and the precessional motion. The off-centered vortex state has been studied through the Gross-Pitaevskii equation [17] and the Thomas-Fermi (TF) approximation [13, 18]. But no solutions of the Bogoliubov equations [1] have thus far been presented for a non-axisymmetric vortex state.

The motivation for an analysis of non-axisymmetric doubly quantized vortex may be explained in a similar way: The instability of the doubly quantized vortex state has been pointed out for the rotationally symmetric vortex state [7]. It relates the existence of a mode with a complex excitation energy and its exponential increase of population. But the axisymmetric state only lasts for an infinitesimal time if the vortex is unstable. It is not known whether the system keeps having the feature (complex eigenvalue) on which the instability of doubly quantized vortex state depends.

This paper presents a two-dimensional analysis of the excitation spectra supported by the condensate with an off-centered vortex, a doubly quantized vortex, and pairs of split vortices. We discuss the above questions of precession, the instability of singly quantized vortex, and the doubly quantized vortex within a unified numerical framework.

## II. SINGLE OFF-CENTERED VORTEX

We consider a two-dimensional  $(x, y)$  system in the rotating frame whose angular velocity is  $\omega$ . The axis of rotation is perpendicular to the  $(x, y)$  plane. Ideally, this represents not only the static condensate in the rotating

---

\*Electronic address: tomoya@focus.hut.fi

vessel but also the precessing vortex. The Hamiltonian is

$$\hat{H}(\boldsymbol{\omega}) = \hat{H} - \boldsymbol{\omega} \cdot \hat{L} \quad (1)$$

$$\hat{H} = \int \hat{\Psi}^\dagger (-C\nabla^2 + V) \hat{\Psi} + \frac{1}{2} g \hat{\Psi}^\dagger \hat{\Psi}^\dagger \hat{\Psi} \hat{\Psi} d\mathbf{r} \quad (2)$$

$$\hat{L} = \int \hat{\Psi}^\dagger (\mathbf{r} \times \mathbf{p}) \hat{\Psi} d\mathbf{r} \quad (3)$$

where  $C = -\hbar^2/(2m)$ ,  $g = 4\pi\hbar^2 a/m$ , and  $V$  is the confining potential with  $a$  denoting the s-wave scattering length and  $m$  the mass. We use  $\boldsymbol{\omega} = (0, 0, \omega)$  and  $\mathbf{r} = (x, y, 0)$ . The time-dependent Gross-Pitaevskii (GP) equation may be written as

$$\begin{aligned} \{-C\nabla^2 + V(x, y) + g|\phi(x, y, t)|^2 \\ - \boldsymbol{\omega} \cdot \mathbf{r} \times \mathbf{p}\} \phi(x, y, t) = i\hbar \frac{\partial \phi(x, y, t)}{\partial t}, \end{aligned} \quad (4)$$

where  $\phi(\mathbf{r})$  is the condensate wavefunction. The time-independent form is

$$\begin{aligned} \{-C\nabla^2 + V(x, y) - \mu + g|\phi(x, y)|^2 \\ - \boldsymbol{\omega} \cdot \mathbf{r} \times \mathbf{p}\} \phi(x, y) = 0, \end{aligned} \quad (5)$$

where  $\mu$  is the chemical potential. We employ an axisymmetric harmonic trapping potential  $V(x, y) = m\omega_{\text{tr}}^2(x^2 + y^2)$  where  $\omega_{\text{tr}} = 2\pi \times 200$ . The linear number density of particles  $N = \int |\phi(\mathbf{r})|^2 d\mathbf{r}$  is fixed to  $1 \times 10^{10} m^{-1}$  in this paper. The mass  $m = 38.17 \times 10^{-27}$  kg and the scattering length  $a = 2.75$  nm for Na atoms are employed.

The angular momentum of the condensate per particle

$$L = \frac{\int \phi^* (\mathbf{r} \times \mathbf{p}) \phi d\mathbf{r}}{\hbar \int |\phi(\mathbf{r})|^2 d\mathbf{r}} \quad (6)$$

is extensively utilized in the following discussion and plotted in several figures. A condensate with a centered vortex has  $L = 1$ . Systems with an off-centered vortex have  $L$  between 0 and 1. We also use the TF radius  $R_{\text{TF}} = 6.79 \mu\text{m}$  as the unit of length.

### A. Static Analysis

The time-dependent Bogoliubov equations [12]

$$\begin{aligned} i\hbar \frac{\partial u(x, y, t)}{\partial t} \\ = (-C\nabla^2 + V - \mu + 2g|\phi|^2 - \boldsymbol{\omega} \cdot \mathbf{r} \times \mathbf{p})u(x, y, t) \\ - g\phi^2 v(x, y, t), \end{aligned} \quad (7)$$

$$\begin{aligned} i\hbar \frac{\partial v(x, y, t)}{\partial t} \\ = -(-C\nabla^2 + V - \mu + 2g|\phi|^2 + \boldsymbol{\omega} \cdot \mathbf{r} \times \mathbf{p})v(x, y, t) \\ + g\phi^{*2}u(x, y, t), \end{aligned} \quad (8)$$

yield the excitation spectra of the condensate which follows the time-dependent GP equation Eq. (4). They reduce to the Bogoliubov equations [1]

$$\begin{aligned} (-C\nabla^2 + V - \mu + 2g|\phi|^2 - \boldsymbol{\omega} \cdot \mathbf{r} \times \mathbf{p})u \\ - g\phi^2 v = \varepsilon u, \end{aligned} \quad (9)$$

$$\begin{aligned} -(-C\nabla^2 + V - \mu + 2g|\phi|^2 + \boldsymbol{\omega} \cdot \mathbf{r} \times \mathbf{p})v \\ + g\phi^{*2}u = \varepsilon v. \end{aligned} \quad (10)$$

when the system is static.

The criteria for the applicability of the Bogoliubov Eqs. (9) and (10), instead of the time-dependent Bogoliubov Eqs. (7) and (8), depends on how fast the wavefunction of the condensate changes. We measure the amplitude of the transformation using

$$V' \equiv \frac{\max(|(-C\nabla^2 + V + g|\phi|^2 - \boldsymbol{\omega} \cdot \mathbf{r} \times \mathbf{p} - \mu)\phi|)}{\hbar \cdot \max(|\phi|)} \quad (11)$$

where the chemical potential  $\mu$  is fixed here [19, 20]. The numerator is a maximum of the left-hand side of Eqs. (4) and (5). Therefore, in the framework of the time-dependent GP equation

$$V'(t) = \max\left(\left|\frac{\partial \phi(x, y, t)}{\partial t}\right|\right) / \max(|\phi(x, y, t)|). \quad (12)$$

For variations of the displacement of the vortex core  $r$ , the  $V'$  has local minima for an axisymmetric vortex state, a vortexfree state, and an off-centered vortex state with certain displacement  $r$  for a choice of  $\omega$ .

We use off-centered vortex states which satisfy

$$V' < 0.0005 \quad (13)$$

in the following analysis of the Bogoliubov equations. Equations (12) and (13) imply that the wavefunction  $\phi$  varies slowly enough in the time scale of the harmonic trap [ $V' < 0.0005 \ll \omega_{\text{tr}}/(2\pi)$ ]. Instead of the right-hand side of Eq. (13), for low values of the angular momentum ( $L < 0.2$ ) the right-hand side is rather relaxed to 0.03.

Each of the relaxation processes, which is numerically equivalent to following the time-dependent GP equation with imaginary time, begins with the TF density profile as the initial configuration on which the phase of an off-centered vortex with various displacements  $r$  is ‘‘imprinted’’ through multiplication. In the beginning of a numerical simulation, the angular velocity  $\omega$  is chosen. Then the development with fixed  $\omega$  is performed without restricting the displacement. The vortex moves freely during the development and ends as an axisymmetric vortex, a vortexfree state, or a vortex state which satisfies Eq. (13). The latter form a set of  $\phi$  and  $\omega$  values which fulfill Eq. (13). Figure 1(a) shows some of the density profiles  $|\phi|^2$  of the condensate. The displacement of the vortex core  $r$  and the angular momentum  $L$  are calculated through Eq. (6) from each of the resulting wavefunctions  $\phi$ . Therefore,  $L$  and  $r$  are functions of  $\omega$

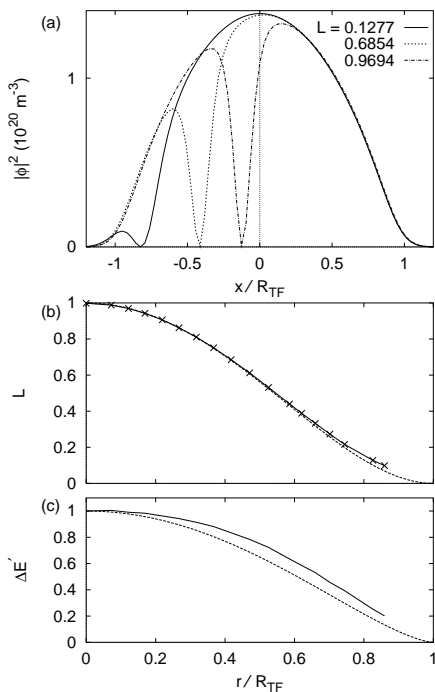


FIG. 1: (a) Density of the condensate along the  $x$ -axis. The angular momenta  $L$  are 0.1277, 0.6854, and 0.9694, respectively. (b) The solid line represents the displacement of a vortex core vs. angular momentum of the condensate per particle. The displacement vanishes for  $L = 1$ . The dotted line is the analytical estimate  $\{1 - (r/R_{\text{TF}})^2\}^2$  by Guilleumas [18]. These two plots overlap in a wide range of displacements,  $0 \leq r < 0.8$ . (c) Displacement of the vortex core  $r$  vs. the normalized additional energy  $\Delta E'$  of the condensate in the presence of an off-centered vortex. The solid line represents the numerical result. The dotted line is obtained by fitting  $\{1 - (r/R_{\text{TF}})^2\}^{3/2}$ , taken from Ref. [21], Eq. (49).

through  $\phi$ . The relation between the angular momentum and the displacement is plotted in Fig. 1(b).

Figure 1(c) displays the normalized additional energy due to the existence of an off-centered vortex, defined through

$$\Delta E' = (E - E_0)/(E_1 - E_0) \quad (14)$$

where  $E_0$ ,  $E_1$ , and  $E$  are the energies of a vortexfree condensate, a condensate in the presence of a centered vortex, and with an off-centered vortex, respectively. If the condensate is vortexfree,  $\Delta E' = 0$ . Off-centered vortex states have  $0 < \Delta E' < 1$  and the centered vortex state has  $\Delta E' = 1$ .

## B. Excitation Spectra

Excitations from a BEC have been interpreted in the framework of the Bogoliubov equations in Ref. [22]. They play a significant role in determining vortex stability.

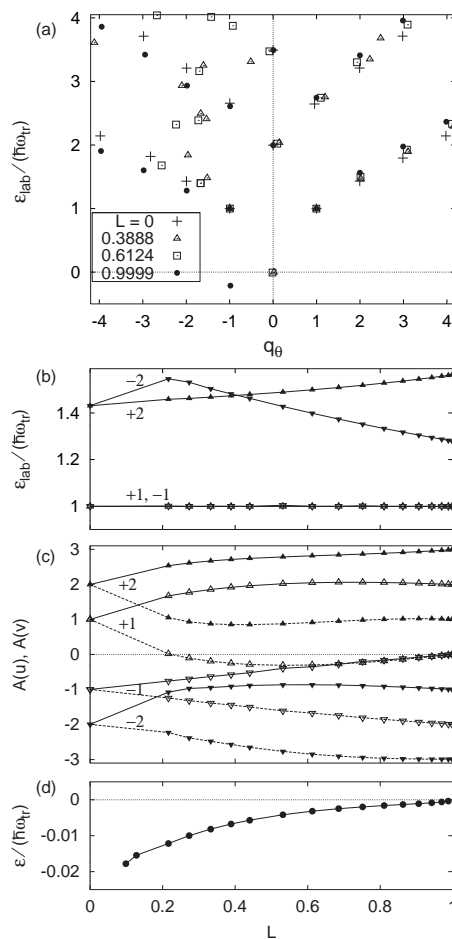


FIG. 2: (a) Excitation spectra of a Bose-Einstein condensate with a centered vortex, an off-centered vortex, and without a vortex. The vertical scale measures the excitation energy,  $\varepsilon_{\text{lab}}$ . The horizontal axis indicates the angular momentum  $q_\theta$ . The crosses, triangles, squares, and the bullets correspond to the angular momenta of the condensate of  $L = 0, 0.38, 0.61$ , and  $1$ , respectively. (b) Excitation energies of the dipole modes (labelled  $+1$  and  $-1$ ) and the quadrupole modes ( $+2$ ,  $-2$ ). (c) The angular momenta of the components  $u$  (solid line) and  $v$  (dotted line) of wavefunction for the dipole ( $+1$ ,  $-1$ ) and quadrupole modes ( $+2$ ,  $-2$ ). (d) Energy  $\varepsilon$  of the lowest core excitation in the rotating frame is negative and it satisfies  $|\varepsilon| \ll 1$ . This is in accordance with the weak instability of the GP equation, Eq. (13).

Nevertheless, these modes in off-centered vortices have not been analyzed so far. An excitation whose energy is  $\varepsilon$  is expressed with two components,  $u$  and  $v$ , of wavefunction each with different momenta. They are determined as the solutions to the eigensystem of Bogoliubov Eqs. (9) and (10). The modes with negative  $\int (|u|^2 - |v|^2) d\mathbf{r}$  are ignored. Two of the lowest excitations are the condensate mode (with  $\varepsilon = 0, u = \phi, v = \phi^*$ ) and the core-localized mode. We ignore the mode with the smallest  $|\varepsilon|$  as the condensate mode.

The wavefunction expressed with  $u$  and  $v$  are obtained

through the Bogoliubov equations (9) and (10). We denote their angular momenta using

$$\mathcal{A}(u) \equiv \frac{\int u^*(\mathbf{r} \times \mathbf{p})u d\mathbf{r}}{\hbar \int |u|^2 d\mathbf{r}}, \quad (15)$$

$$\mathcal{A}(v) \equiv \frac{\int v^*(\mathbf{r} \times \mathbf{p})v d\mathbf{r}}{\hbar \int |v|^2 d\mathbf{r}}. \quad (16)$$

These quantities correspond to the angular momentum of the condensate  $L$  defined in Eq. (6). Some algebra with the help of Eqs. (5), (9), and (10) shows that the excitation energies  $\varepsilon$  depend linearly on  $\omega$ . We presume that the wavefunctions  $\phi$ ,  $u$ , and  $v$  do not depend on  $\omega$  and energies  $\mu$  and  $\varepsilon$  do not have imaginary part. The coefficient of proportionality is

$$q_\theta \equiv \frac{\text{Re} [\{\mathcal{A}(u) - L\} \int |u|^2 d\mathbf{r} + \{\mathcal{A}(v) + L\} \int |v|^2 d\mathbf{r}]}{\int (|u|^2 + |v|^2) d\mathbf{r}}. \quad (17)$$

We introduce an excitation energy in the laboratory frame

$$\varepsilon_{\text{lab}} \equiv \varepsilon + \hbar\omega q_\theta. \quad (18)$$

Equation (17) includes  $\mathcal{A}(u)$ ,  $\mathcal{A}(v)$ , and  $L$  because an excitation level has two components  $u$  and  $v$  of wavefunction and their phases are always affected by the phase of the condensate. For axisymmetric systems, the  $q_\theta$  definition reduces to an integer quantum number [9, 10]. The excitation energies  $\varepsilon$  and  $\varepsilon_{\text{lab}}$  are normalized by the trap unit  $\hbar\omega_{\text{tr}}$  from here on. Figure 2(a) displays the computed excitation energies,  $\varepsilon$ , and the corresponding angular momenta,  $q_\theta$ . Some of the modes, for example those with  $(\varepsilon_{\text{lab}}, q_\theta) = (2, 0), (1, \pm 1)$  maintain similar values of  $q_\theta$  and  $\varepsilon_{\text{lab}}$  upon variations of  $L$ . We call the modes at  $(2, 0)$  and  $(1, \pm 1)$  the breathing [1] and the dipole modes, respectively. Some of the core-localized modes have  $(\varepsilon_{\text{lab}}, q_\theta) = (0, 0)$ . These are discussed in Sec. II C. The modes with  $(\varepsilon_{\text{lab}}, q_\theta) \simeq (1, \pm 1), (1.5, \pm 2)$  are discussed in Sec. II D.

### C. Core-Localized Mode

For any value of  $L$ , the system has one core-localized mode. The modes always displays a sharp peak in the amplitude  $|u|^2 + |v|^2$  of the wavefunction at the vortex core. The core-localized modes still feature a major difference between the system with  $L = 1$  and those with  $0 < L < 1$ .

When  $L = 1$ , the vortex is in the center of the system. The angular momentum  $q_\theta = -1$  and the excitation energy  $\varepsilon_{\text{lab}}$  is negative [the lowest bullet at  $q_\theta = -1$  in Fig. 2(a)]. It has a sharp peak in the vortex core. The sharp localization, the angular momentum, and the negative energy are equivalent with those for axisymmetric calculations [9, 10].

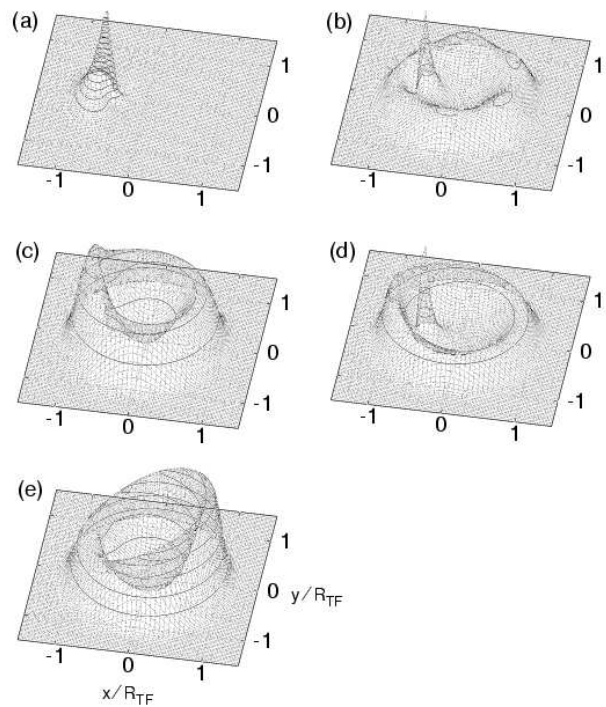


FIG. 3: Wavefunctions  $|u|^2$  of (a) the core-localized mode, (b) dipole mode with negative  $q_\theta$ , (c) dipole mode with positive  $q_\theta$ , (d) quadrupole mode with negative  $q_\theta$ , and (e) quadrupole mode with positive  $q_\theta$ . Solid lines denote contours of density. The core-localized mode has a peak of the amplitude in the vortex core. The peak in the quadrupole mode with negative  $q_\theta$  is not seen in axisymmetric systems. The angular momentum  $L$  of the condensate is 0.531.

Once the vortex becomes off-centered ( $0 < L < 1$ ), both of the components  $u$  and  $v$  of the wavefunction localize in the vortex core [Fig. 3(a)]. Each of them features a sharp peak in the vortex core and its skirt extends towards the surface of the condensate. The angular momenta  $\mathcal{A}(u)$  of the core-localized modes vary between 1 and 4. The corresponding wavefunctions  $v$  have opposite angular momenta. Their average  $q_\theta$  almost vanishes ( $|q_\theta| \ll 1$ ); the points at  $(0,0)$  in Fig. 2(a) mean this. The excitation energy plotted in Fig. 2(d) remains below zero ( $-0.01 < \varepsilon < 0$ ) even in the rotating frame.

The core-localized mode behaves differently between the system with  $L = 1$  and that with  $0 < L < 1$ . One possible cause is the static approximation of the time-dependent Bogoliubov equations introduced in Sec. II A. While the system with  $L = 1$  is treated with the Bogoliubov equations, systems with  $0 < L < 1$  are described within the time-dependent Bogoliubov equations.

### D. Dipole and Quadrupole Modes

Excitations having the lowest positive energy at  $q_\theta = \pm 1$  and  $\simeq \pm 2$  are classified as the dipole and quadrupole

modes. Figure 2(b) shows the energy for these modes. The energies of the dipole modes almost equal one trap unit ( $\hbar\omega_{\text{tr}}$ ). The dipole modes are known to be responsible for the center-of-mass motion [23]. Therefore, they are not affected by various profiles inside the condensate. The angular momenta  $\mathcal{A}(u)$  and  $\mathcal{A}(v)$  are plotted in Fig. 2(c). These excitations show continual transformation as a function of variation of the vortex displacement.

The condensate in a two-dimensional harmonic potential has two quadrupole modes. The splitting between the quadrupole frequencies  $\varepsilon_{\text{lab}}(+2) - \varepsilon_{\text{lab}}(-2)$  is inverted at  $L \leq 0.4$ , while it is proportional to  $L$  in systems with a centered vortex [23]. The corresponding eigenoscillation of the condensate, called the scissors mode, has been observed experimentally [24] to measure an angular momentum of the condensate. The inversion may affect the observations of the angular momentum.

Guilleumas *et al.* [18] estimate the splitting using several methods within the TF limit. Their Eqs. (33) and (42) and our numerical results in Fig. 2(b) agree well when the vortex is close to the axis ( $r/R_{\text{TF}} < 0.2$ ). Their estimates stay positive and approach zero as the displacement of the vortex approaches  $R_{\text{TF}}$ . But the sign is inverted in our numerical results. This is caused by an increase of the energy  $\varepsilon_{\text{lab}}(-2)$  at lower  $L$ , depicted in Fig. 2(b). The wavefunction  $u$  of the  $-2$  mode displays a sharp peak at the vortex center; for example, in Fig. 3(d). This peak is significant for lower  $L$  and not seen in the axisymmetric (non)vortex states. We presume that the existence of this peak is pushing up the energy  $\varepsilon_{\text{lab}}(-2)$ .

For  $\omega \gtrsim 0.35\omega_{\text{tr}}$  (corresponding to  $L < 0.2$ ), the excitation energies of the modes with  $q_\theta > 2$  approach each other, and their wavefunctions become numerically indistinguishable from one another. The angular momenta of the excitations in this region ( $L < 0.2$ ) are omitted in Figs. 2 for the sake of clarity.

### III. TWO VORTICES

A vortex with the winding number two has been formed in a condensate of Na atoms [5]. Multiply quantized vortices are energetically unfavorable against the array of the singly quantized vortices (e.g. Sec. 9.2.1 in Ref. [1]), while the experimental data does not indicate any signs of the splitting. In this section, we investigate the excitation spectra of systems with two vortices to inspect their stability in the splitting process.

Each of the GP calculations starts from an initial wavefunction with two slightly displaced vortices under a fixed angular velocity  $\omega$ , which acts as an external adjustable parameter. The initial wavefunction is formed from the TF density profile in the absence of a vortex, but multiplied with the phase factor  $e^{i\theta}$  around each of the initial vortex positions. The resulting angular momenta are controlled through this  $\omega$ . The GP equation has a static solution for about  $60 < \omega/(2\pi) < 110$ .

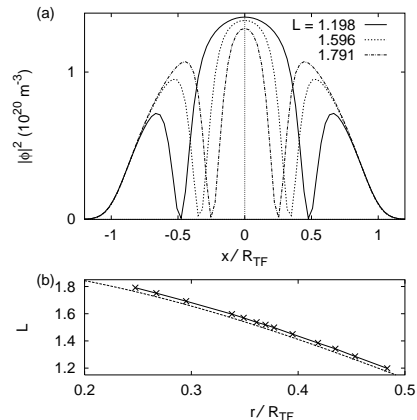


FIG. 4: (a) Density of condensate along  $x$ -axis. A condensate has two vortices and both of them are on the  $x$ -axis. Angular momenta  $L$  are 1.198, 1.596, and 1.791, respectively. (b) Displacement of vortex core vs. angular momentum of the condensate per particle. The displacement will be zero when the angular momentum of the condensate is 2. The dotted line is the analytical estimate  $2\{1 - (r/R_{\text{TF}})^2\}^2$  taken from Eq. (24) in Ref. [18]. The two plots agree well.

The corresponding range of angular momenta is from 1.2 to 1.8. Many vortices enter into the condensate for higher  $\omega/(2\pi) > 110$  and the vortices disappear for  $\omega/(2\pi) < 60$ . Figure 4 shows density profiles of the condensate for various angular momenta.

Using the condensate wavefunctions, the excitations from it are calculated with the Bogoliubov equations, Eqs. (9) and (10). We found that one or two conjugate pairs of modes with complex eigenvalues always exists in the calculated range of  $L$ .

Figure 5(d) shows the energy levels for two excitations with the lowest real part in the rotating frame. For  $1.2 < L < 1.57$ , there occur two conjugate pairs of complex eigenvalues, both of them have a large imaginary part. For larger  $L$ , only one of them has a large imaginary part. Figure 6 displays the wavefunctions of these lowest modes. One of them has an imaginary eigenvalue, while the other one has a real eigenvalue. Both of them display a peak in the vortex core.

A doubly quantized vortex in a rotationally symmetric system has two negative excitations, those for  $q_\theta = -1$  and  $-2$ . One of them with  $q_\theta = -2$  sometimes has a complex energy, depending on the particle density in the system, see Ref. [7]. This feature is equivalent to those of our results depicted in Fig. 5(d) for higher  $L$ . Therefore, the splitted vortices keep on having unstable nature which exist before the splitting [7].

Figure 5(a) shows that the modes with positive energy stay with similar values of  $\varepsilon_{\text{lab}}$  and  $q_\theta$  as functions of the separation of the vortices. The lowest positive-energy modes, with  $q_\theta \simeq \pm 1$  and  $q_\theta \simeq \pm 2$ , are classified as the dipole and quadrupole modes. Their computed

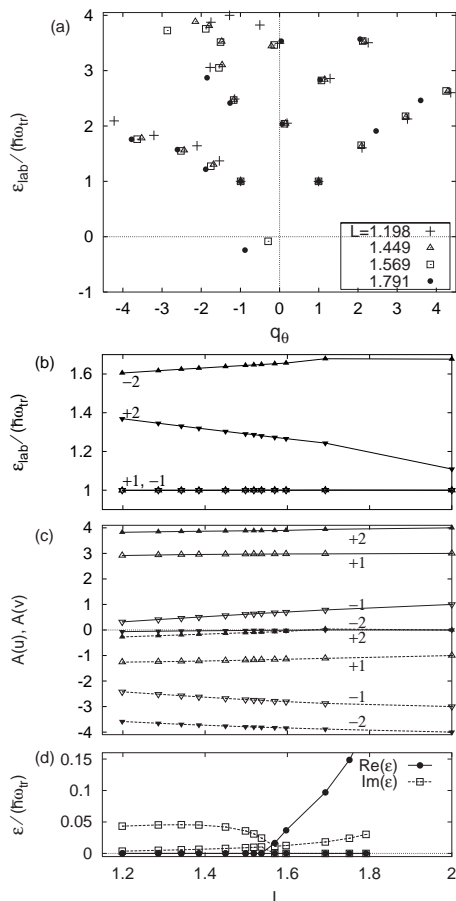


FIG. 5: (a) Excitation spectra of a Bose-Einstein condensate with a pair of off-centered vortices. The vertical axis denotes the excitation energy,  $\varepsilon_{\text{lab}}$ . The modes with complex energies are not plotted here because the definitions of  $\varepsilon_{\text{lab}}$  and  $q_\theta$  in Eqs. (17) and (18) do not support modes with complex energies. The horizontal axis is the angular momentum,  $q_\theta$ . The crosses, triangles, squares, and bullets correspond to the angular momenta of the condensate 1.198, 1.449, 1.569, and 1.791, respectively. (b) Energy levels  $\varepsilon_{\text{lab}}$  of the quadrupole and dipole modes in the laboratory frame. (c) Angular momenta of the quadrupole and dipole modes. Solid lines show those of  $u$ , while the dashed lines correspond to  $v$ . (d) Two excitations with the lowest  $\text{Re}(\varepsilon)$ . Conjugate modes with negative imaginary parts are not plotted. A system has two conjugate pairs of complex eigenvalues or one pair of complex eigenvalues and one real eigenvalue. The real and imaginary parts are plotted independently. The points at  $L = 2$  in (b) and (c) are taken from axisymmetric calculations.

angular momenta and energies in the laboratory frame are presented in Fig. 5(b) and 5(c). The modes near  $(q_\theta, \varepsilon_{\text{lab}}) = (0, 2)$  are breathing modes. The consistent behavior of the dipole, quadrupole, and breathing modes throughout the results in systems with an off-centered vortex [Figs. 2(a)-2(c)], two vortices [Figs. 5(a)-5(c)], and an axisymmetric vortex ( $L = 1, 2$ ) proves the validity of our numerical procedure.

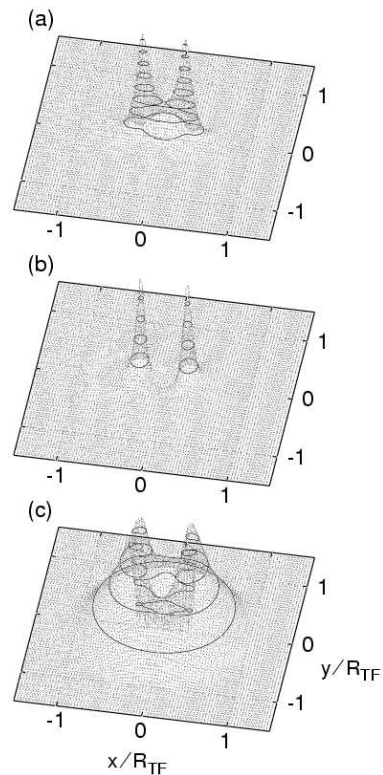


FIG. 6: (a) Wavefunction  $|u|^2$  of a complex mode; the wavefunction  $v$  of the complex mode is the conjugate of  $u$ . The energy levels of these modes are  $\pm 0.0241i$ . (b) (c) Wavefunctions  $|u|^2$  and  $|v|^2$  of the lowest mode. The energy eigenvalue of this mode is  $\varepsilon_{\text{lab}} = -0.2329$ . The angular momentum of the condensate is 1.750.

#### IV. PRECESSION FREQUENCIES

The above results are calculated in the rotating frame. It is not self-evident whether they may be interpreted as results for precessing vortices in the laboratory frame. To estimate the validity of the condensate wavefunction, we carry out time-dependent Gross-Pitaevskii calculations in the laboratory frame. The above results of the static GP equation are allowed to evolve in time according to Eq. (4).

The condensate shows precessional motion of the vortices for both the single-vortex and the two-vortex cases. Figure 7 shows the precessional angular velocity,  $\omega_{\text{pr}}$ . The rotation frequency  $\omega$  that we obtained in the static calculations in Secs. II and III are also plotted. The two frequencies agree well. It means that our results in the rotating frame can also be identified as those in the laboratory frame. The excitation modes, including the core mode, precess following the vortex core there.

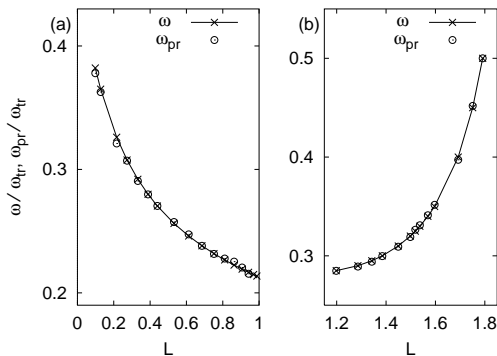


FIG. 7: Circles represent the precessional angular velocities according to time-dependent calculations; lines show the angular velocity  $\omega/\omega_{tr}$  that gives each value of angular momentum  $L$ . The vertical axis is normalized by the trap frequency. (a) Systems with one vortex. (b) Two vortices.

## V. DISCUSSION

The excitation spectra of Bose Einstein condensates with one and two off-centered vortices has been computed. The excitation with negative energy and localization at the vortex core always exists not only in the axisymmetric state but also for the off-centered vortex configurations. We depicted the shape of wavefunctions and excitation energy of the core-localized, dipole and quadrupole modes in the off-centered vortex states with both one and two vortices. The invariance of dipole and breathing modes in the nonaxisymmetric cases shows that usage of the Bogoliubov equation instead of the time-dependent Bogoliubov equation is valid.

The rotation frequencies agree well with the precession

frequencies of vortices in the laboratory frame. It enables us to consider the two problems, precession of the vortices and the vortex instability concerning the negative excitation, independently. The precessing vortices pursue to have a core-localized excitation with negative excitation energy in the framework of Bogoliubov equations. Therefore, the condensate with one precessing vortex maintains the instability as long as the vortex exists. In order to pose an answer to the problem [16] between the precessing mode and the instability, this work is to be extended to treat finite-temperature systems [9, 11].

Concerning the splitting of the doubly quantized vortex, the existence of two core-localized excitations is confirmed throughout the calculated range of  $L$ . The vortex pair always has an instability [7, 25] because systems with a vortex pair always support core excitations with complex excitation energies, *c.f.* Fig. 5(d).

Throughout the analyses, the system displays two quadrupole excitations. The excitation energies of the quadrupole modes Figs. 2(b) and 5(b) are useful because these excitation is used to measure the angular momenta of the condensate experimentally.

## Acknowledgements

Authors thank CSC Scientific Computing Ltd (Finland) for computer resources. We are grateful to M. Möttönen, M. Nakahara, C. J. Pethick, T. P. Simula, and S. M. M. Virtanen for stimulating discussions. One of the authors (TI) is supported by the bilateral exchange programme between the Academy of Finland and the Japan Society for the Promotion of Science.

- 
- [1] C. J. Pethick and H. Smith, *Bose-Einstein Condensation in Dilute Gases* (Cambridge University Press, Cambridge, England, 2002).
  - [2] M. R. Matthews, B. P. Anderson, P. C. Haljan, D. S. Hall, C. E. Wieman, and E. A. Cornell, Phys. Rev. Lett. **83**, 2498 (1999).
  - [3] B. P. Anderson, P. C. Haljan, C. E. Wieman, and E. A. Cornell, Phys. Rev. Lett. **85**, 2857 (2000).
  - [4] K. W. Madison, F. Chevy, W. Wohlleben, and J. Dalibard, Phys. Rev. Lett. **84**, 806 (2000).
  - [5] A. E. Leanhardt, A. Görlitz, A. P. Chikkatur, D. Kielpinski, Y. Shin, D. E. Pritchard, and W. Ketterle, Phys. Rev. Lett. **89**, 190403 (2002).
  - [6] M. Nakahara, T. Isoshima, K. Machida, S.-i. Ogawa, and T. Ohmi, Physica B **284**, 17 (2000); T. Isoshima, M. Nakahara, T. Ohmi, and K. Machida, Phys. Rev. A **61**, 063610 (2000); S.-i. Ogawa, M. Möttönen, M. Nakahara, T. Ohmi, and H. Shimada, Phys. Rev. A **66**, 013617 (2002); M. Möttönen, N. Matsumoto, M. Nakahara, and T. Ohmi, J. Phys.: Cond. Matt. **14**, 29 (2002).
  - [7] H. Pu, C. K. Law, J. H. Eberly, and N. P. Bigelow, Phys. Rev. A **59**, 1533 (1999).
  - [8] R. J. Dodd, K. Burnett, M. Edwards, and C. W. Clark, Phys. Rev. A **56**, 587 (1997).
  - [9] T. Isoshima, K. Machida, Phys. Rev. A **59**, 2203 (1999);
  - [10] T. Isoshima, K. Machida, Phys. Rev. A **60**, 3313 (1999).
  - [11] S. M. M. Virtanen, T. P. Simula, and M. M. Salomaa, Phys. Rev. Lett. **86**, 2704 (2001).
  - [12] S. M. M. Virtanen, T. P. Simula, and M. M. Salomaa, Phys. Rev. Lett. **87**, 230403 (2001). The time-dependent Hartree-Fock-Bogoliubov-Popov equations reduces to time-dependent Bogoliubov equations at zero temperature.
  - [13] A. A. Svidzinsky and A. L. Fetter, **84**, 5919 (2000).
  - [14] M. Linn and A. L. Fetter, Phys. Rev. A **61**, 063603 (2000).
  - [15] D. L. Feder, A. A. Svidzinsky, A. L. Fetter, and C. W. Clark, Phys. Rev. Lett. **86**, 564 (2001).
  - [16] S. M. M. Virtanen, T. P. Simula, and M. M. Salomaa, J. Phys: Condens. Matter **13**, L819 (2001).

- [17] D. A. Butts and D. S. Rokhsar, *Nature* **397**, 327 (1999).
- [18] M. Guilleumas and R. Graham, *Phys. Rev. A* **64**, 033607 (2001).
- [19] The chemical potential  $\mu$  is fixed for each of the procedures to obtain the condensate wavefunction. The procedure is repeated with slightly different value of  $\mu$  until the result gives the total particle number  $N = 1 \times 10^{10} \text{ m}^{-1}$ .
- [20] The denominator  $\max(|\phi|)$  of Eq. (11) does not vary much [see peaks of densities in Figs. 1(a)] because the trapping potential is fixed and the chemical potential  $\mu$  is chosen such that the particle number  $N$  becomes close to  $N = 1 \times 10^{10} \text{ m}^{-1}$ . So the denominator works as a normalization factor for the amplitude of the condensate wavefunction.
- [21] A. L. Fetter and A. A. Svidzinsky, e-print cond-mat/0102003.
- [22] J. M. Vogels, K. Xu, C. Raman, J. R. Abo-Shaeer, and W. Ketterle, *Phys. Rev. Lett.* **88**, 060402 (2002).
- [23] F. Zambelli and S. Stringari, *Phys. Rev. Lett.* **81**, 1754 (1998).
- [24] F. Chevy, K. W. Madison, and J. Dalibard, *Phys. Rev. Lett.* **85**, 2223 (2000).
- [25] D. V. Skryabin, *Phys. Rev. A* **63**, 013602 (2000).